Research Paper

EPHA5 mutations predict survival after immunotherapy in lung adenocarcinoma

Zhiming Chen[1,*], Ji Chen[2,*], Dandan Ren[3,*], Jiao Zhang[3], Ying Yang[3], Henghui Zhang[4], Beibei Mao[3], Haitao Ma[1]

[1]Department of Thoracic Surgery, The First Affiliated Hospital of Soochow University, Suzhou, Jiangsu Province, China
[2]Department of Thoracic Surgery, Huashan Hospital, Shanghai, China
[3]Genecast Precision Medicine Technology Institute, Beijing, China
[4]Institute of Infectious Diseases, Beijing Ditan Hospital, Capital Medical University, Beijing Key Laboratory of Emerging Infectious Diseases, Beijing, China
*Equal contribution

Correspondence to: Haitao Ma, Beibei Mao; **email:** mahaitao@suda.edu.cn, mao.beibei@genecast.com.cn
Keywords: immunotherapy, lung adenocarcinoma, EPHA5, TMB, PDL1
Received: June 10, 2020 **Accepted:** October 3, 2020 **Published:** December 3, 2020

ABSTRACT

Eph receptors constitute the largest family of RTKs, and their associations with antitumor immunity and immunotherapy are largely unknown. By integrating genomic, transcriptomic and clinical data from cohorts in public databases, we identified EPHA5 as the most common mutated gene of Eph receptors in lung adenocarcinoma (LUAD). Moreover, compared with EPHA5 wild-type (WT) patients, EPHA5-mutant (Mut) patients exhibited significantly enhanced infiltration of $CD8^+$ T cells and M1 macrophages, reduced recruitment of immunosuppressive regulatory T cells (Tregs) into the tumor site, as well as the increased level of chemokine, interferon-gamma, inhibitory immune checkpoint signatures, tumor mutation burden (TMB) and tumor neoantigen burden (TNB). Additionally, EPHA5 mutation cooccurred with homologous recombination (HR) or mismatch repair (MMR) gene mutations. These data were validated in the LUAD cell line H1299 and a Chinese LUAD cohort. Most importantly, clinical analysis of a Memorial Sloan Kettering Cancer Center (MSKCC) immunotherapy cohort indicated that LUAD patients with EPHA5 mutations who were treated with immunotherapy had markedly prolonged survival times.
Our results revealed the correlation of EPHA5 mutations with tumor immune microenvironment and predictive factors for immunotherapy, implying the potential of EPHA5 mutations as a prognostic marker for the prognosis of LUAD patients to immune checkpoint blockade therapy.

INTRODUCTION

Lung cancer is the leading cause of cancer-related death worldwide [1] and is classified mainly as small cell lung cancer (SCLC) and non-SCLC (NSCLC). On the basis of histological parameters, NSCLC is classified as lung adenocarcinoma (LUAD), lung squamous cell carcinoma (LUSC) and large cell carcinoma.

Small molecule protein kinase inhibitors targeting tyrosine kinases, including epidermal growth factor receptor (EGFR) and anaplastic lymphoma kinase (ALK), have been widely used to improve the prognosis of advanced NSCLC patients with genetic alterations in these targeted genes [2, 3]. Patients expressing the wild-type (WT) form of these tyrosine kinases may derive therapeutic benefit from compounds that target immune checkpoints such as programmed death-1 (PD-1) and programmed death ligand-1 (PD-L1) [4]. For example, pembrolizumab, which targets PD-1, is approved by the Food and Drug Administration (FDA) for treating advanced NSCLC patients without mutations in EGFR

or ALK and with high PD-L1 expression [5]. However, a large proportion of cancer patients do not respond to this therapy. Substantial evidence indicates that the response to cancer immunotherapy is closely related to PD-L1 expression [6], the tumor mutation burden (TMB) [7] and tumor-infiltrating lymphocytes (TILs) [8]. In addition, in NSCLC, mutations in specific genes may be correlated with the immunotherapy response, e.g., commutation of TP53 and KRAS improves the response of patients to anti-PD-1 therapy [9].

Eph receptors constitute the largest family of receptor tyrosine kinases (RTKs). In vertebrates, this family has 16 members, namely, EphA receptors 1-10 (EphA1-A10) and EphB receptors 1-6 (EphB1-B6) [10]. Upon binding of their Ephrin ligands, these receptors transduce external signals into cells through the Src, RAS/MAPK, and integrin pathways and control a variety of biological processes related to tumor progression [11–13]. Eph receptors are also expressed on cells of the immune system, and Eph-ephrin interactions have been reported to mediate immune cell activation, migration, adhesion, and proliferation [14–16]. However, publications regarding the relationship of Eph receptors with the tumor immune microenvironment are limited. In a recent study, researchers found that knockout of EphA10 reduced the expression of PDL1 in breast cancer cells [17]. This finding prompted us to explore the relevance of Eph receptors to antitumor immunity in the tumor microenvironment (TME).

In this study, we performed an integrated analysis incorporating DNA sequencing and RNA sequencing (RNA-seq) data from the LUAD dataset in The Cancer Genome Atlas (TCGA) database and a Chinese cohort to determine the correlations of Eph receptor mutations with antitumor immunity in LUAD by a bioinformatics approach. We found that mutation of EPHA5, the most frequently mutated gene in the Eph receptor family, was associated with $CD8^+$ T cell infiltration, intratumoral PD-L1 expression, increased TMB and mutations in DNA damage response (DDR) pathway genes. Significantly, we revealed that the survival of EPHA5-mutant (Mut) LUAD patients was more favorable than that of EPHA5-WT patients in an immunotherapy setting, providing new insight into the search for predictive biomarkers for the immunotherapy response in lung cancer.

RESULTS

EPHA5 mutations are associated with enhanced immunity in LUAD

Before investigating the association between Eph receptors and antitumor immunity, we first determined the mutational landscape of different Eph receptors in LUAD patients in the TCGA database. As shown in Figure 1, 239/566 patients had mutations in Eph family members. EPHA5 was the most frequently mutated gene (13%), followed by EPHA3 (9%). The mutation frequencies of other Eph family members were lower than 10% (Figure 1A). To ensure that a sufficient number of patients with mutations were included in subsequent statistical analyses, we selected EPHA5, with a mutation frequency of higher than 10%, to examine the relationship of EPHA5 mutations with tumor immune microenvironment.

TILs play an essential antitumor role in the TME. CIBERSORT analysis of the RNA-seq data from the TCGA LUAD dataset showed increased recruitment of $CD8^+$ T cells and M1 macrophages and reduced recruitment of immunosuppressive cells, e.g., regulatory T cells (Tregs), in EPHA5-Mut samples (Figure 1B). Next, we evaluated the association between EPHA5 mutations and immune signatures. As shown in Figure 2A, EPHA5 mutations were correlated with significantly increased expression of the interferon-gamma (IFN-γ) signature genes as well as the chemokine signature genes, which has been suggested to be related to the immunotherapy response [18]. Among the 6 genes in the IFN-γ signature, the expression levels of only IDO1 and HLA-DRA were not distinct; those of the other 4 genes—IFN-γ and the chemokines CXCL9, CXCL10, and CXCL11were higher in EPHA5-Mut samples. Additionally, the expression of GZMA, an important factor in the cytolytic activity signature, had more abundance in EPHA5-Mut samples. Notably, we evaluated the expression of immune checkpoint genes and found that the expression of inhibitory checkpoint molecules, such as LAG3 and PDL1 (CD274), was higher in the EPHA5-Mut group than in the EPHA5-WT group (Figure 2B).

The TME has been proposed to be classified into four types based on the presence of PDL1 (CD274) and $CD8^+$ TILs [19]. Samples in which the PDL1 and CD8A/CD8B expression levels above the corresponding median RNA expression levels were defined as positive. The EPHA5-Mut group contained a higher proportion of $PDL1^+/CD8^+$ samples than the EPHA5-WT group (Figure 2C), indicating that the EPHA5-Mut population is more likely to benefit from immune checkpoint blockade (ICB) therapy than the EPHA5-WT population.

To further elucidate the association between EPHA5 and antitumor immunity, we knocked down the expression of EPHA5 in H1299 cells. siRNA-mediated depletion of EPHA5 in H1299 cells decreased the

enrichment of interferon-γ (IFN-γ) and the nuclear factor kappa B (NF-κB) signaling pathway components which are responsible for the expression of PDL1 (CD274) [20, 21] (Figure 3A–3C). Further real-time PCR analysis revealed that knockdown of EPHA5 in H1299 cells downregulated the expression of PDL1 (CD274), IDO1 and CXCL10 (Figure 3D).

EPHA5 mutations are associated with elevated TMB and TNB in LUAD.

TMB has been reported to be associated with various immune signatures [22]. Given the evidence that EPHA5 mutations were associated with the tumor immune microenvironment, we sought to determine whether EPHA5 mutations are correlated with TMB. In the TCGA LUAD cohort, EPHA5-Mut patients had a significantly higher TMB than EPHA5-WT patients (Figure 4A). Similarly, in the Memorial Sloan Kettering Cancer Center (MSKCC) immunotherapy cohort (Supplementary Table 1), EPHA5-Mut LUAD cancers also exhibited a significantly higher TMB than EPHA5-WT LUAD cancers, indicating a convincing association between EPHA5 mutations and TMB (Figure 4B).

Neoantigens can be derived from tumor somatic mutations. Considering that EPHA5-Mut patients had a higher number of somatic mutations, we assessed TNB in different groups. Consistent with the pattern of somatic mutations, an immunogenic TNB was more common in patients with EPHA5 mutations than in patients without EPHA5 mutations (Figure 4C). This difference may explain the more abundant infiltration of TILs in the EPHA5-Mut TME than in the EPHA5-WT TME, as these mutated neoantigens can be recognized by TILs and induce tumor-specific immune responses.

Uncontrolled cell cycle progression induced by oncogene hyperactivation and DNA replication stress causes replication fork arrest and DNA damage [23].

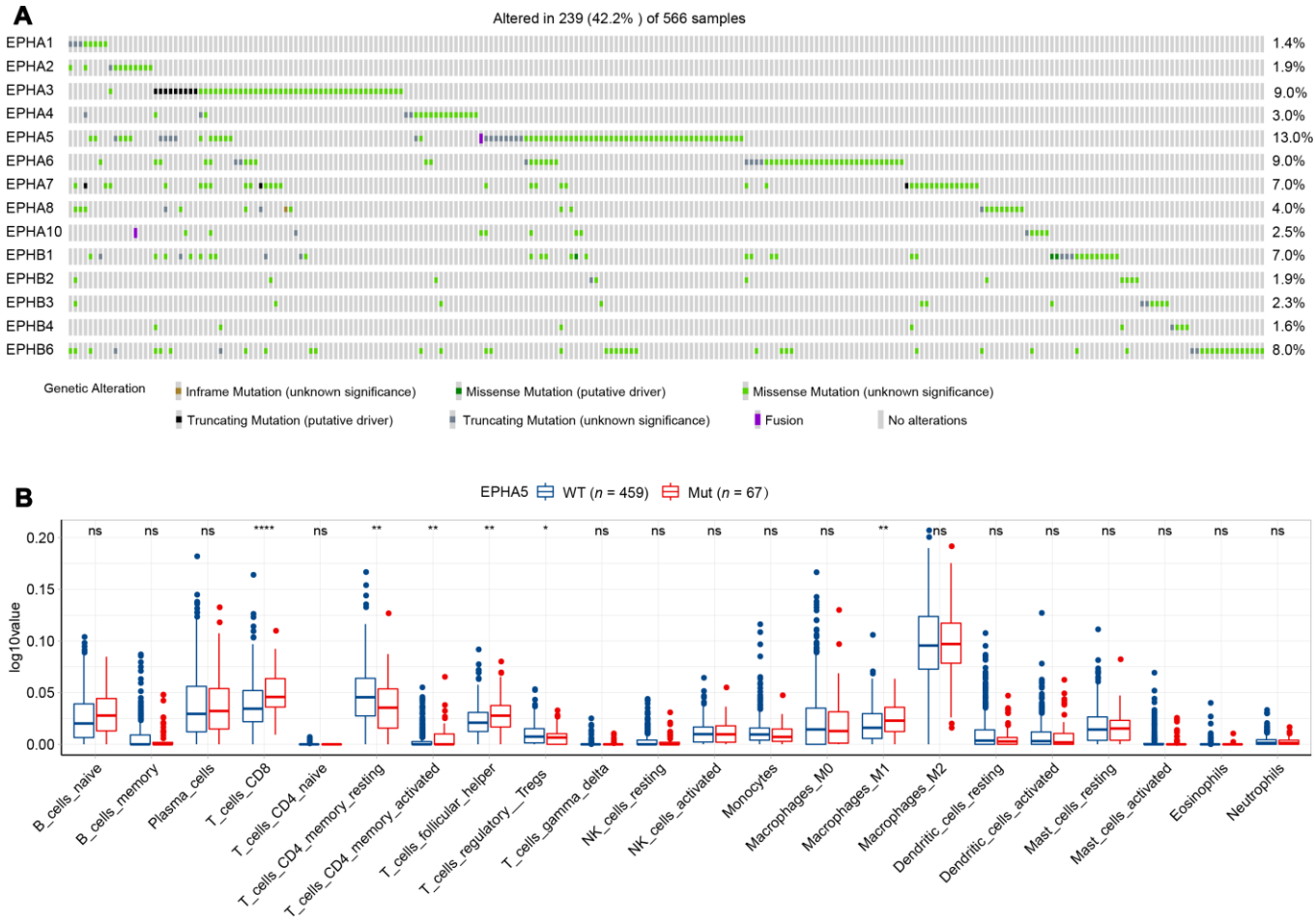

Figure 1. EPHA5 mutations and immune infiltration are correlated in the TCGA LUAD cohort. (**A**) Mutational oncoplot of the Eph family in LUAD. (**B**) Comparison of immune infiltration between EPHA5-Mut and EPHA5-WT tumors. The ordinate log10value represents log10(cibersort score+1).

Combined with DDR deficiency, unrepaired DNA damage tends to generate tumor mutations. Herein, gene set enrichment analysis (GSEA) revealed that EPHA5 mutations were accompanied with accelerated cell cycle progression and increased DNA replication (Figure 4D). Additionally, we discovered significantly increased mutation frequencies for genes in the homologous recombination repair (HR) and mismatch repair (MMR) pathways (Figure 4E, Supplementary Table 2).

Then, we collected the formalin-fixed, paraffin-embedded (FFPE) samples of 143 Chinese LUAD

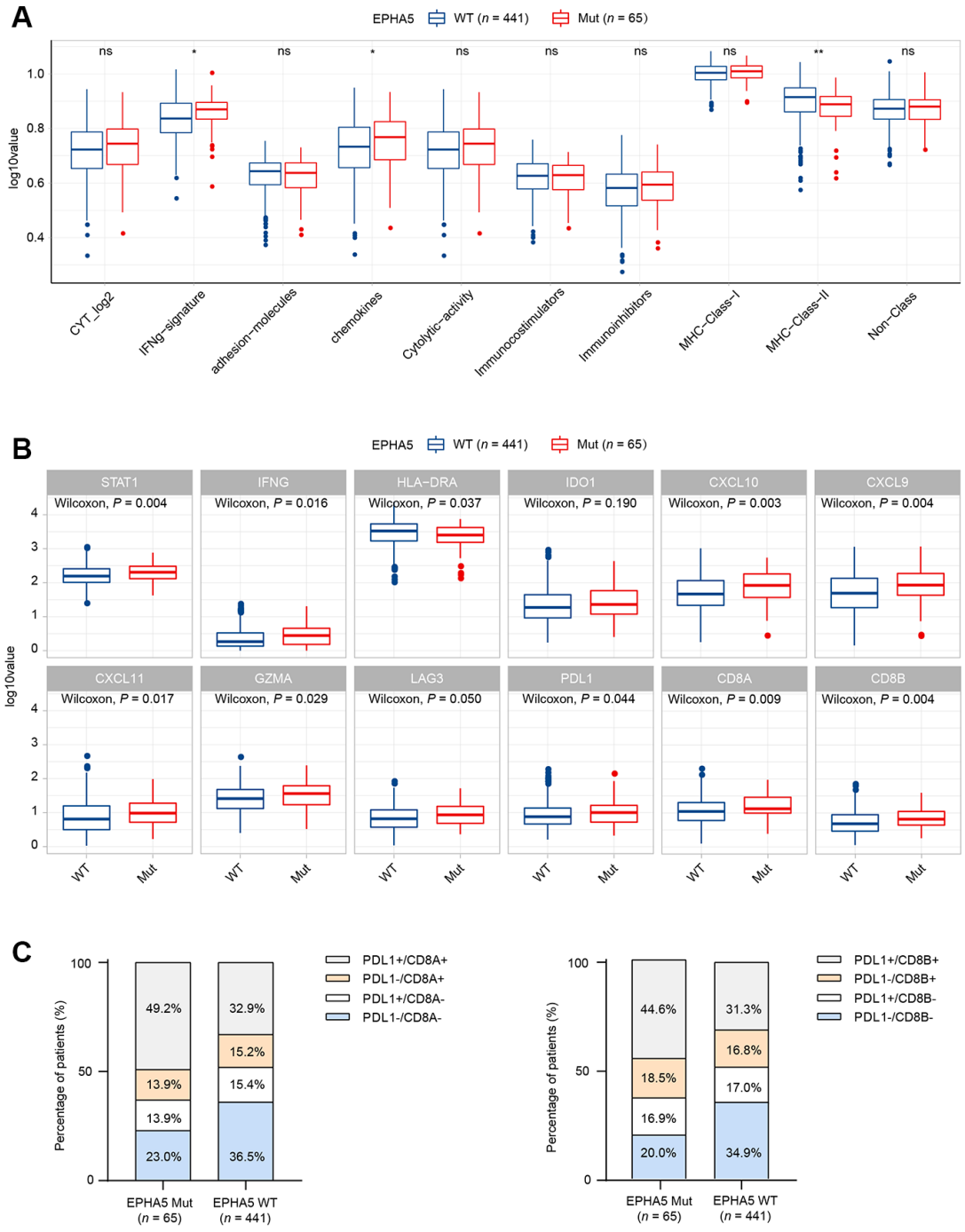

Figure 2. Alterations in EPHA5 are associated with enhanced immunity in the TCGA LUAD cohort. (**A**) IFN-γ and chemokine signatures were enriched in EPHA5-Mut tumors. The ordinate log10value represents log10(ssGSEA score+1). (**B**) The expression levels of immune checkpoint inhibitor genes were significantly higher in EPHA5-Mut tumors than in EPHA5-WT tumors. The ordinate log10value represents log10(TPM+1). (**C**) A higher proportion of $PDL1^{+}/CD8^{+}$ cells was observed in EPHA5-Mut tumors than in EPHA5-WT tumors.

patients and performed targeted DNA sequencing with a 543-gene panel. Analysis of the mutational profile showed that the frequency of EPHA5 mutations (6.3%, 9/143, Figure 5A) in the Chinese cohort was slightly lower than that in the TCGA cohort and the MSKCC immunotherapy cohort. Despite the low EPHA5 mutation frequency in the Chinese cohort, patients with EPHA5 mutations had a significantly higher TMB (range from 0 to 34.3 mutations/Mb) than patients with WT EPHA5 (Figure 5B). Similarly, mutations in HR or MMR pathway genes occurred concurrently with EPHA5 (Figure 5C–5E), indicating that EPHA5 mutations accompanied by deficiencies in DNA repair pathways tend to cause accumulation of mutations in tumors.

EPHA5 mutations are associated with favorable prognosis after ICB therapy in patients with LUAD

High PDL1 expression, high TMB, high $CD8^+$ T cell infiltration and the IFN-γ signature are well-documented predictive biomarkers for the response to immunotherapy [8]. The associations between EPHA5 and these biomarkers indicated that EPHA5 mutation alone is likely a novel predictor for the response to ICB therapy. Thus, we examined this hypothesis in the MSKCC immunotherapy cohort of LUAD patients. Consistent with the results described above, EPHA5-Mut patients had significantly more favorable overall survival (OS) than EPHA5-WT patients after immunotherapy (Figure 6A). Similarly, in the MSKCC pancancer cohort of patients treated with immunotherapy, EPHA5-Mut patients had significantly more favorable OS than EPHA5-WT patients (Figure 6B). However, in the cohorts of patients from the TCGA LUAD and MSKCC pancancer cohorts who were not treated with immunotherapy, no significant difference in OS was observed between EPHA5-Mut and WT patients (Figure 6C, 6D), suggesting that the prognostic value of EPHA5 mutation is specific for patients treated with immunotherapy. In another advanced non-squamous NSCLC cohort of patients

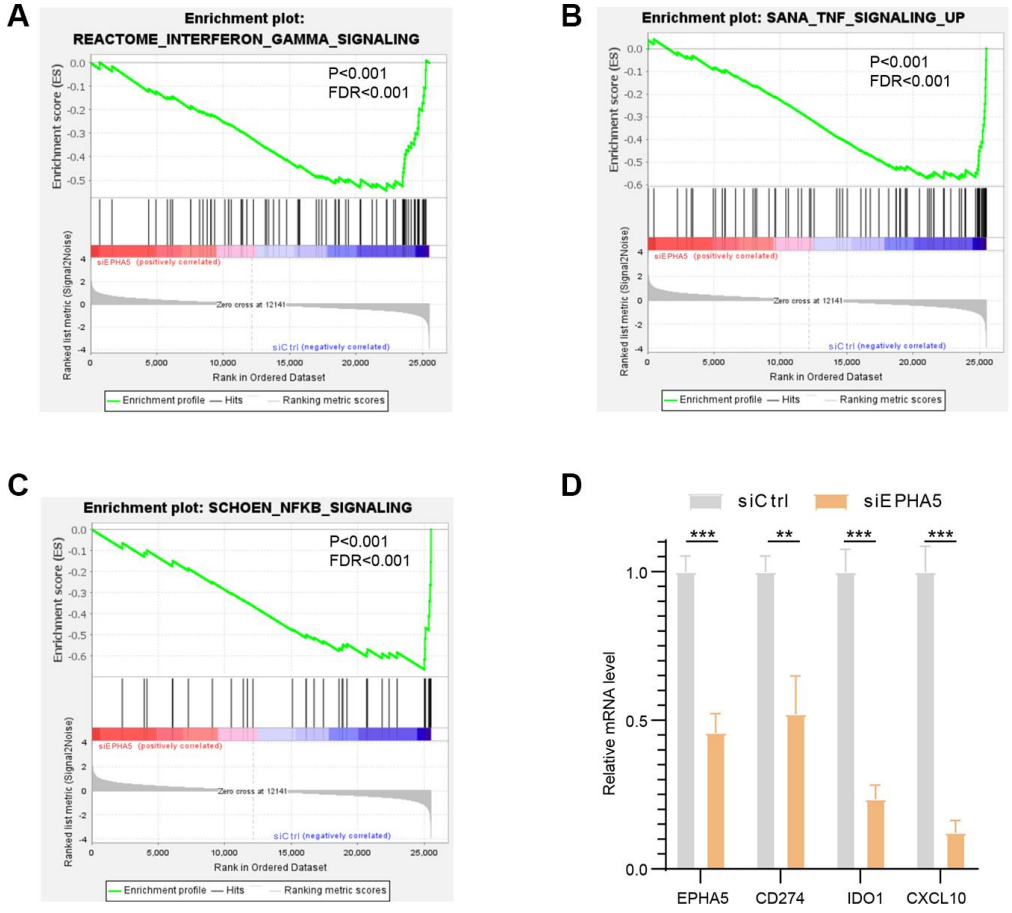

Figure 3. Knockdown of EPHA5 in H1299 cells impaired immune related pathways enrichment and expression of immune checkpoint genes. EPHA5 depletion in H1299 cells reduced the enrichment of (**A**) IFN-γ, (**B**) TNF, and (**C**) NF-κB signaling pathway components. (**D**) EPHA5 KD in H1299 cells downregulated the expression of PDL1 (CD274), IDO1 and CXCL10. **: $P < 0.01$, ***: $P < 0.001$.

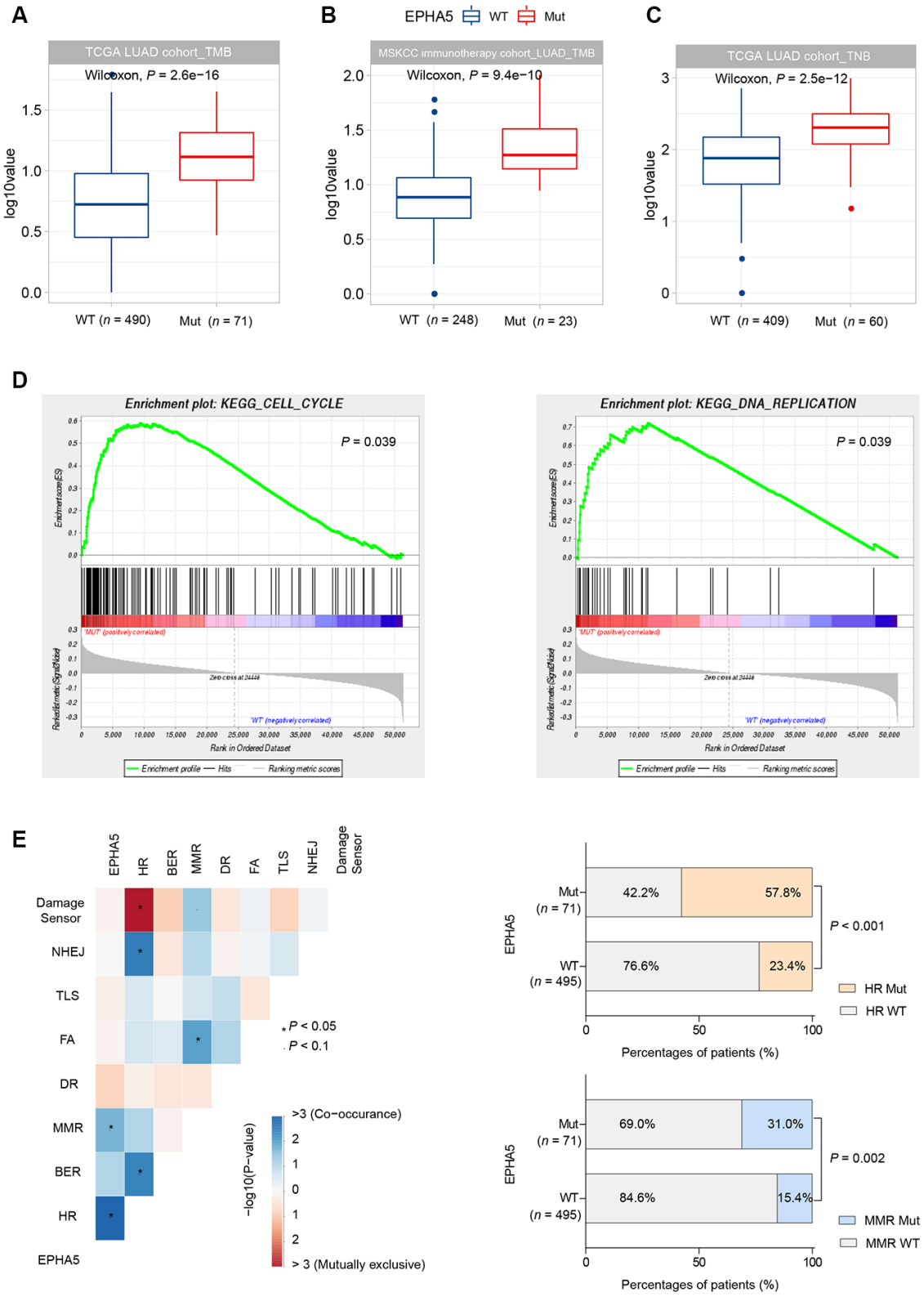

Figure 4. EPHA5 mutations are related to increased TMB and TNB in LUAD. EPHA5-Mut tumors had a markedly higher TMB than EPHA5-WT tumors in both the (**A**) TCGA LUAD cohort and (**B**) MSKCC immunotherapy LUAD cohort. The ordinate log10value represents log10(TMB+1). (**C**) In the TCGA LUAD cohort, EPHA5-Mut tumors had an increased immunogenic TNB. The ordinate log10value representslog10(TNB+1). (**D**) EPHA5 mutations were positively correlated with enrichment of the cell cycle and DNA replication pathways in the TCGA LUAD cohort. (**E**) Significantly increased mutation frequencies of genes in the HR and MMR pathways were observed in EPHA5-Mut tumors in the TCGA LUAD cohort.

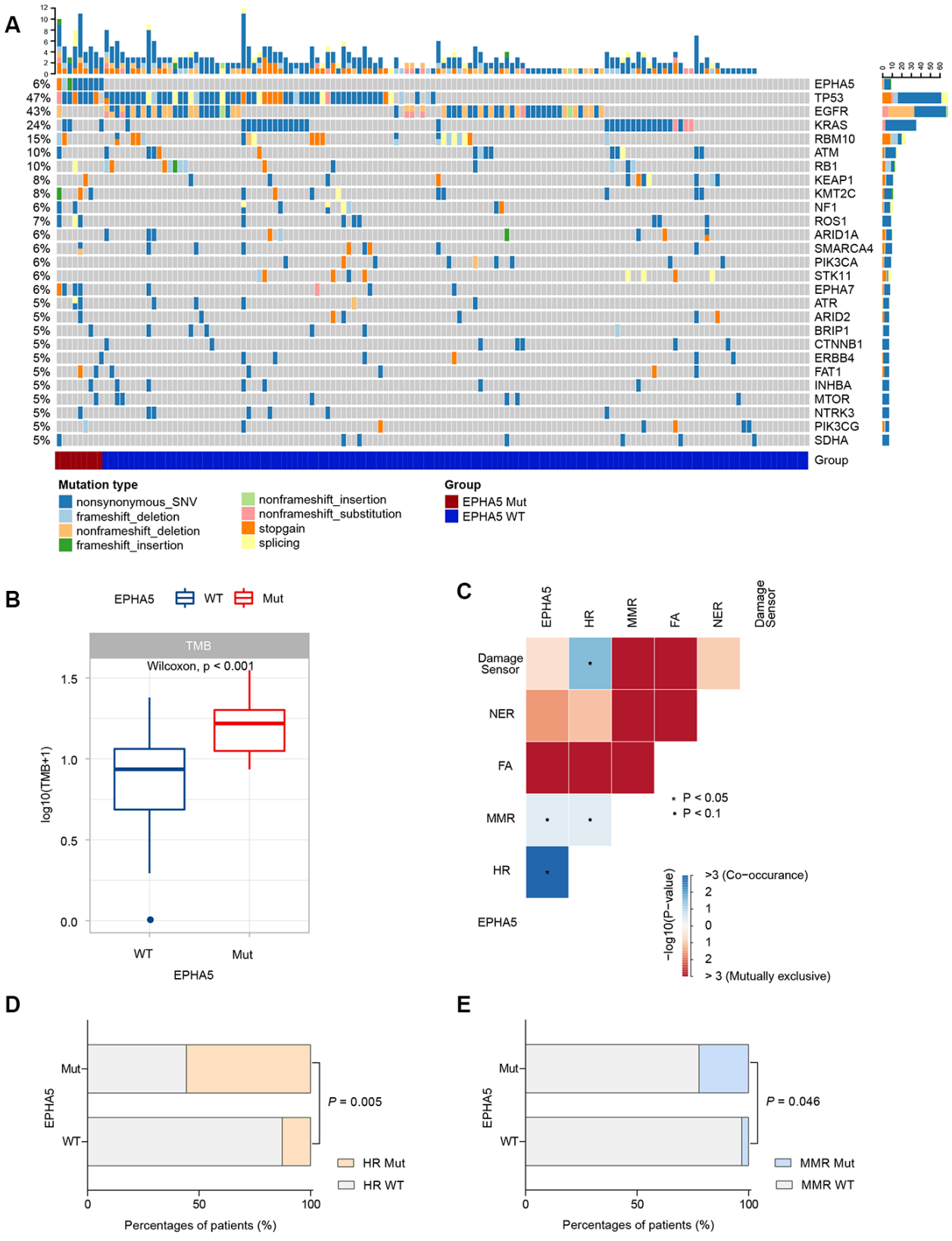

Figure 5. EPHA5 mutation is correlated with increased TMB and occurred concurrently with DNA repair pathways in Chinses LUAD patients. (**A**) Mutational landscape of the Chinese LUAD cohort. (**B**) EPHA5-Mut tumors had a markedly higher TMB than EPHA5-WT tumors. (**C**) EPHA5 mutations occurred concurrently with HR and MMR pathways. Markedly higher proportion of (**D**) HR and (**E**) MMR pathway mutations were observed in EPHA5-Mut group.

treated with immunotherapy (Hellmann Cohort [24], Supplementary Table 3), all patients with EPHA5 mutation (nonsynonymous_snv) presented durable clinical benefit (Supplementary Figure 1A) and had high TMB (TMB > 314 mutations, i.e., the top 25% of patients, Supplementary Figure 1B). Moreover, the EPHA5-Mut group had and tended to have longer progression-free survival times (Supplementary Figure 1), further confirming the role of EPHA5 mutation as a potential prognostic factor for the response to immunotherapy.

Additionally, in the MSKCC immunotherapy cohort, patients with high TMB (TMB > 10.82 mutations/Mb, i.e., the top 25% of patients) had more favorable OS than those with low TMB (Figure 6E). However, higher TMB did not confer longer OS times than low TMB in patients without EPHA5 mutation (Figure 6F). Conversely, patients with both high TMB and mutation of EPHA5 had the best outcomes in terms of the response to immunotherapy, suggesting that the combination of EPHA5 mutation and high TMB is a more precise biomarker than either alone for selecting the patients most likely to benefit from immunotherapy.

DISCUSSION

The Eph family of receptors is the largest family of RTKs. Overexpression or hyperactivation of Eph receptors has been found in cells from various cancers [25–27]. Most previous studies have focused on the role of Eph in regulating intrinsic characteristics that facilitate cancer progression. Less is known about the association of Eph receptors on antitumor immunity. Our study, for the first time, addressed the association between Eph receptor mutations and the tumor immune microenvironment via integrated analysis of WES and RNA-seq data from the TCGA LUAD cohort. Our analysis showed that EPHA5 mutation has a significant positive association with antitumor immunity, including increased infiltration of adaptive and innate lymphocytes and enriched IFN-γ and cytolytic activity signatures. Moreover, EPHA5-Mut LUAD tumors displayed higher TMB than EPHA5-WT tumors in both the TCGA and Chinese cohorts. Consistent with these preclinical predictions, clinical analysis based on the MSKCC immunotherapy cohort confirmed the potential of EPHA5 mutation as a prognostic biomarker for the immunotherapy response.

The “cancer-immunity cycle” proposed by Chen and Mellman begins with the release of tumor cell antigens [28]. Among the Eph receptor family members, EphA2 and EphA3 have been identified as tumor-associated antigens (TAAs), and their epitopes can be recognized by both $CD4^+$ and $CD8^+$ T cells [29, 30]. EphA2 has also been reported to regulate immune cell trafficking. Two other receptors, EphA1 and EphA4, are expressed in T cells and mediate T cell chemotaxis *in vitro* [31–33]. Although no evidence currently suggests that EPHA5 is a TAA, our results showed that mutations in EPHA5 were associated with increased TMB and TNB. During the subsequent steps of the cancer-immunity cycle, EPHA5 mutations likely do not correlate with TAA presentation, as the MHC-I signature did not differ between patients with WT EPHA5 and those with mutated EPHA5. However, components of the chemokine signature, including CXCL9, CXCL10 and CXCL11, which are responsible for immune cell migration, differentiation, and activation [34], were enriched in EPHA5-Mut patients, leading to infiltration of cytotoxic T cells. More importantly, EPHA5 mutations were correlated with high expression levels of checkpoint inhibitors such as LAG3 and PDL1, suggesting that mutations in EPHA5 were accompanied by $CD8^+$ T cell exhaustion in LUAD. Notably, we validated the impact of EPHA5 on the expression of PDL1, IDO and CXCL10 in H1299 cells. Thus, for the first time, we identified the link between EPHA5 and the tumor immune microenvironment in LUAD. However, this relationship requires further validation in mouse models.

Numerous studies have demonstrated that immunotherapy, especially with inhibitors of PD-1 or PDL1, has improved the prognosis of NSCLC patients and reformed therapeutic strategies for NSCLC [4, 7, 35]. Currently, several biomarkers that predict drug sensitivity or resistance have been identified, including TMB, $CD8^+$ T cell infiltration into the TME and intratumoral PDL1 expression as evaluated by immunohistochemistry (IHC) [8]. Although the detection of biomarkers can identify patients who may benefit from immunotherapy, not all patients with high TMB or high expression of PDL1 respond well [36]. Other challenges, such as appropriate definition of cutoff values, limit the clinical application of these biomarkers. Thus, identification of biomarkers representing two or more of the above factors is needed to guide immunotherapy applications. Our findings that EPHA5 mutation was correlated with high TMB, high PDL1 expression, high CD8+ cell infiltration and high expression of IFN-γ signature components in LUAD imply that EPHA5 mutations can predict most of the current features related to the immunotherapy response in LUAD.

Moreover, we found a higher proportion of $TIL^+PD\text{-}L1^+$ patients among EPHA5-Mut patients than among EPHA5-WT patients, supporting the conclusion that EPHA5-Mut patients treated with PDL1 blockade therapy are likely to exhibit a relatively good prognosis.

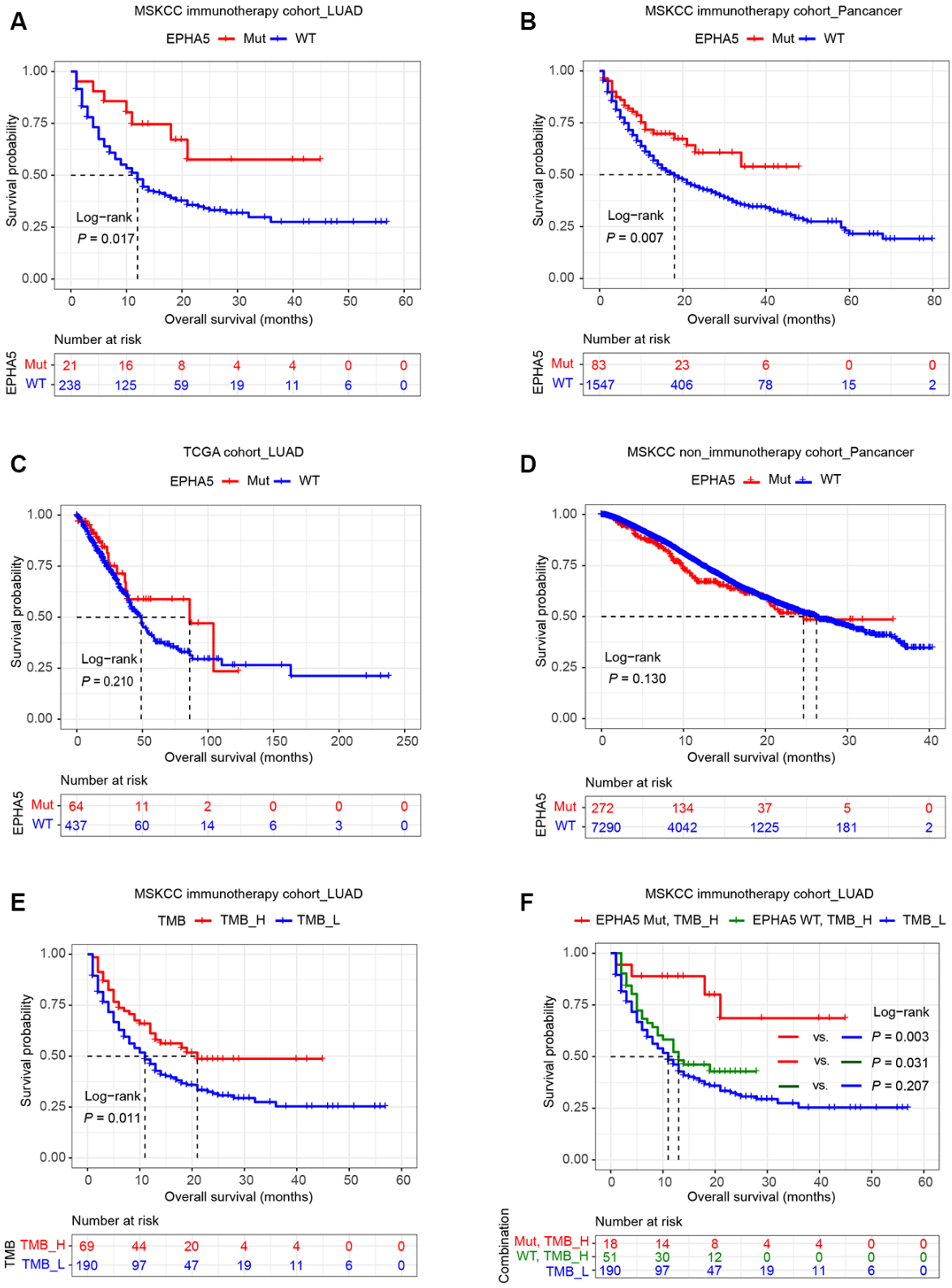

Figure 6. Relation of EPHA5 to clinical outcomes in LUAD. Patients with tumors harboring EPHA5 mutations had longer OS times than those with tumors without EPHA5 mutations in the MSKCC immunotherapy cohort: (**A**) LUAD set, (**B**) pancancer set. The OS time did not differ significantly between EPHA5-Mut and EPHA5-WT patients not treated with immunotherapy in the (**C**) TCGA LUAD or (**D**) MSKCC pancancer cohort. (**E**) High tumor mutation burden (TMB_H) was positively correlated with prolonged OS in the MSKCC immunotherapy cohort. (**F**) Survival curves were generated for patients in the MSKCC immunotherapy cohort stratified by both the EPHA5 mutation status and the TMB. *P*-values calculated with the log-rank test are shown.

Most importantly, although patients with high TMB (25% top) had longer OS times than patients with low TMB, the subgroup of EPHA5-WT patients with high TMB had OS times equivalent to those of patients with low TMB. Thus, detection of the EPHA5 mutation status may help prevent overtreatment of EPHA5-WT patients with high TMB and avert the development of immune-related adverse effects in these patients.

This study has several limitations. First, we established the relationship between EPHA5 and antitumor immunity based only on data from tumor specimens. More in-depth studies using mouse model- or cell culture-based techniques are needed to confirm our findings. Second, validation of the prognostic or predictive role of EPHA5 mutations for the immunotherapy response is necessary in an independent cohort of ICB-treated patients. In conclusion, we discovered the obvious importance of EPHA5 mutations in increasing TMB, T cell infiltration into the TME and PDL1 expression, implying that EPHA5 mutation is a potential prognostic marker for the immunotherapy response.

MATERIALS AND METHODS

Data acquisition

Three LUAD genomic datasets were utilized in this study: the genomic dataset from the MSK-IMPACT clinical sequencing cohort pancancer study (MSKCC, Nat Med 2017), a LUAD dataset (TCGA, PanCancer Atlas) and an MSKCC immunotherapy cohort (Nat Genet 2019). The gene expression profiling data for the LUAD dataset (TCGA, PanCancer Atlas) were downloaded from the GDC data portal (https://portal.gdc.cancer.gov/). Fragments per kilobase million mapped reads (FPKM) values in RNA-seq data were transformed into transcripts per kilobase million (TPM) values.

Evaluation of immune cell infiltration and immune gene signatures

The abundances of 22 immune cell types were calculated with CIBERSORT [37]. The gene sets for cytolytic activity (granzyme-A and perforin-1), the IFN-γ signature, immune costimulators, immune inhibitors, chemokines, the HLA-I signature (MHC-class I), and the HLA-II (MHC-class II) signature were analyzed as described in previous studies [18, 38].

TNB and TMB data were obtained from published TCGA data [39]. Somatic alterations in ten oncogenic signaling pathways were determined as described in previously published literature [40].

Patient information

A total of 143 LUAD patients were recruited from The First Affiliated Hospital of Soochow University. Clinically recorded information, such as age, sex, smoking status, and pathologic stage, was collected as shown in Supplementary Table 4. All patients provided written informed consent for molecular analysis of their tissue samples.

This study was approved by the Ethics Committee of the First Affiliated Hospital of Soochow University. All procedures in studies involving human participants were performed in accordance with the ethical standards of the institutional and/or national research committee and with the 1964 Helsinki Declaration and its later amendments or with comparable ethical standards.

DNA extraction and sequencing

FFPE tumor specimens and matched blood samples were collected and submitted to construct the designed 543-gene NGS panel (Supplementary Table 5) for testing based on next-generation sequencing (NGS). DNA extraction and sequencing were performed using standard protocols described previously [41].

Variant analysis

To identify somatic single nucleotide variants (SNVs) and indels, matched blood samples from patients were used as controls for the FFPE tumor samples with mutations. SNVs were called with VarDict (version 1.5.1) [42]. Variants were annotated with ANNOVAR [43]. Variants that met one or more of the following criteria were excluded: (a) < 30× sequencing coverage, (b) silent mutations in nonreference alleles, (c) < 5 supporting reads, (d) an allele frequency of ≥0.005 in the Exome Aggregation Consortium (ExAC) or Genome Aggregation Database (gnomAD), or (e) an allele frequency of <0.02 in the tumor sample. TMB (mutations/Mb) was calculated with the previously reported algorithm [44].

Cell culture and transfection

H1299 cells were grown in RPMI 1640 medium (Gibco) supplemented with 10% FBS and 1% penicillin-streptomycin (Invitrogen). Cells were maintained at 37° C in an atmosphere containing 5% CO_2.

Transient knockdown of the Epha5 gene was performed by transfection of siRNA with Lipofectamine® RNAiMAX Transfection Reagent (#13778150, Invitrogen). The siRNA (siEPHA5) targeted the following sequence: catctccagtcaccaatgtga.

RNA isolation and RT-qPCR

Cultured cells were lysed with TRIzol™ Reagent (#15596018, Invitrogen). Total RNA was isolated according to the manufacturer's instructions. mRNA was reverse transcribed to cDNA with a cDNA synthesis kit (AE311-03, TransGen Biotech, Beijing, China). RT-qPCR was performed with diluted cDNA (1:4) in three wells per reaction with the appropriate primer pair and SYBR green master mix (Bio-Rad) in a Bio-Rad iCycler iQ Real Time PCR System. All RT-qPCR experiments were repeated at least three independent times. The primer sequences are listed below: Human IDO1-F: GCCAGCTTCGAGAAA GAGTTG; Human IDO1-R: ATCCCAGAACTAGA CGTGCAA; Human CD274-F: TGGCATTTGCTGA ACGCATTT; Human CD274-R: TGCAGCCAGGTC TAATTGTTTT; Human CXCL10-F: GTGGCATTC AAGGAGTACCTC; Human CXCL10-R: TGATGGC CTTCGATTCTGGATT; Human EPHA5-F: GTGACC GATGAACCTCCCAAA; Human EPHA5-R: CCAG GTCTGCACACTTGACAG; Human beta-Actin-F: TG ACAGGATCGAGAAGGAGA; Human beta-Actin-R: CGCTCAGGAGGAGCAATG.

RNA sequencing

RNA was quantified using a Life Invitrogen Qubit 3.0/4.0 fluorometer and assessed using an Agilent 2100 Bioanalyzer system. Then, 8 μl of total RNA was used as input with a SMARTer Stranded Total RNA-Seq Kit v2 (Takara) in accordance with the low-throughput protocol. After PCR enrichment and purification of adapter-ligated fragments, the library with adapters was analyzed with the Life Invitrogen Qubit 3.0/4.0 and assessed in the Agilent 2100 Bioanalyzer system. Then, RNA-seq was performed on a Illumina NovaSeq 6000 Sequencing System. To ensure data quality, raw reads were preprocessed by removing low-quality sequences, removing junction contamination (with Trimmomatic) [45], detecting the A/T/G/C content distribution (with RSeQC) [46], removing rRNA (with bowtie2) [47], etc., to obtain high-quality sequences (clean reads). All subsequent analyses were based on clean reads. Reference gene and genome annotation files were downloaded from the GENCODE website (https://www.gencodegenes.org/human/). Clean data were aligned to the reference genome with HISAT [48] (http://ccb.jhu.edu/software/hisat2/index.shtml). FeatureCounts was used to estimate the expression level of each gene. Gene expression was quantified with the FPKM method [49].

GSEA

GSEA (http://software.broadinstitute.org/gsea/index.jsp) was conducted based on the expression results by using the default parameters on c2 gene sets in the Molecular Signatures Database (MSigDB) (http://software.broadinstitute.org/gsea/msigdb).

Statistical analysis

For two-group comparisons, statistical significance was estimated with unpaired Student's t tests for normally distributed variables and with the Mann-Whitney U test for nonnormally distributed variables. Fisher's exact test for pairwise comparisons was performed to detect sets of pathways mutually exclusive or cooccurring with EPHA5. Fisher's exact test was also used to compare the proportions of mutations in HR and MMR genes between the EPHA5-Mut and EPHA5-WT groups. The Kaplan-Meier method was used to generate survival curves for the subgroups in each dataset, and the log-rank (Mantel-Cox) test was used to determine the statistical significance of the differences. Statistical analyses were performed in R (https://www.r-project.org/, version 3.6.1), and $P < 0.05$ was considered to indicate a statistically significant difference.

Ethics approval

This study was performed in accordance with the ethical standards and the Declaration of Helsinki and according to national and international guidelines. Surgically procured tumor samples from patients were obtained in the Department of Thoracic Surgery, The First Affiliated Hospital of Soochow University with informed patients' consent for research purposes.

Abbreviations

NSCLC: non-small cell lung cancer; LUAD: lung adenocarcinoma; SCLC: small cell lung cancer; LUSC: lung squamous cell carcinoma; EGFR: epidermal growth factor receptor; ALK: anaplastic lymphoma kinase; IFN-γ: interferon-γ; NF-κB: nuclear factor kappa B; TNF: tumor necrosis factor; RTKs: receptor tyrosine kinases; Tregs: regulatory T cells; MSKCC: Memorial Sloan Kettering Cancer Center; TCGA: The Cancer Genome Atlas; PD-1: programmed death-1; PD-L1: programmed death ligand-1; TMB: tumor mutation burden; TILs: tumor-infiltrating lymphocytes; TNB: tumor neoantigen burden; HR: homologous recombination; MMR: mismatch repair.

AUTHOR CONTRIBUTIONS

BB M and ZM C conceived and designed this study. ZM C collected the specimens and clinical data. JC performed the cell line experiments. BBM, DD R, JZ and YY analyzed the data and interpreted of results. ZM

C, BB M and DD R drafted the manuscript. BB M, HH Z and HT M provided critical comments, suggestions and revised the manuscript. All authors read and approved the final version of the manuscript.

CONFLICTS OF INTEREST

The authors declare no conflicts of interest.

FUNDING

This work was supported by the National Natural Science Foundation of China (81672281).

REFERENCES

1. Bray F, Ferlay J, Soerjomataram I, Siegel RL, Torre LA, Jemal A. Global cancer statistics 2018: GLOBOCAN estimates of incidence and mortality worldwide for 36 cancers in 185 countries. CA Cancer J Clin. 2018; 68:394–424. https://doi.org/10.3322/caac.21492 PMID:30207593

2. Soria JC, Ohe Y, Vansteenkiste J, Reungwetwattana T, Chewaskulyong B, Lee KH, Dechaphunkul A, Imamura F, Nogami N, Kurata T, Okamoto I, Zhou C, Cho BC, et al, and FLAURA Investigators. Osimertinib in untreated EGFR-mutated advanced non-small-cell lung cancer. N Engl J Med. 2018; 378:113–25. https://doi.org/10.1056/NEJMoa1713137 PMID:29151359

3. Camidge DR, Kim HR, Ahn MJ, Yang JC, Han JY, Lee JS, Hochmair MJ, Li JY, Chang GC, Lee KH, Gridelli C, Delmonte A, Garcia Campelo R, et al. Brigatinib versus crizotinib in ALK-positive non-small-cell lung cancer. N Engl J Med. 2018; 379:2027–39. https://doi.org/10.1056/NEJMoa1810171 PMID:30280657

4. Reck M, Rodríguez-Abreu D, Robinson AG, Hui R, Csőszi T, Fülöp A, Gottfried M, Peled N, Tafreshi A, Cuffe S, O'Brien M, Rao S, Hotta K, et al, and KEYNOTE-024 Investigators. Pembrolizumab versus chemotherapy for PD-L1-positive non-small-cell lung cancer. N Engl J Med. 2016; 375:1823–33. https://doi.org/10.1056/NEJMoa1606774 PMID:27718847

5. Pai-Scherf L, Blumenthal GM, Li H, Subramaniam S, Mishra-Kalyani PS, He K, Zhao H, Yu J, Paciga M, Goldberg KB, McKee AE, Keegan P, Pazdur R. FDA approval summary: pembrolizumab for treatment of metastatic non-small cell lung cancer: first-line therapy and beyond. Oncologist. 2017; 22:1392–99. https://doi.org/10.1634/theoncologist.2017-0078 PMID:28835513

6. Topalian SL, Hodi FS, Brahmer JR, Gettinger SN, Smith DC, McDermott DF, Powderly JD, Carvajal RD, Sosman JA, Atkins MB, Leming PD, Spigel DR, Antonia SJ, et al. Safety, activity, and immune correlates of anti-PD-1 antibody in cancer. N Engl J Med. 2012; 366:2443–54. https://doi.org/10.1056/NEJMoa1200690 PMID:22658127

7. Hellmann MD, Ciuleanu TE, Pluzanski A, Lee JS, Otterson GA, Audigier-Valette C, Minenza E, Linardou H, Burgers S, Salman P, Borghaei H, Ramalingam SS, Brahmer J, et al. Nivolumab plus ipilimumab in lung cancer with a high tumor mutational burden. N Engl J Med. 2018; 378:2093–104. https://doi.org/10.1056/NEJMoa1801946 PMID:29658845

8. Lu S, Stein JE, Rimm DL, Wang DW, Bell JM, Johnson DB, Sosman JA, Schalper KA, Anders RA, Wang H, Hoyt C, Pardoll DM, Danilova L, Taube JM. Comparison of biomarker modalities for predicting response to PD-1/PD-L1 checkpoint blockade: a systematic review and meta-analysis. JAMA Oncol. 2019; 5:1195–204. https://doi.org/10.1001/jamaoncol.2019.1549 PMID:31318407

9. Dong ZY, Zhong WZ, Zhang XC, Su J, Xie Z, Liu SY, Tu HY, Chen HJ, Sun YL, Zhou Q, Yang JJ, Yang XN, Lin JX, et al. Potential predictive value of TP53 and KRAS mutation status for response to PD-1 blockade immunotherapy in lung adenocarcinoma. Clin Cancer Res. 2017; 23:3012–24. https://doi.org/10.1158/1078-0432.CCR-16-2554 PMID:28039262

10. Kania A, Klein R. Mechanisms of ephrin-eph signalling in development, physiology and disease. Nat Rev Mol Cell Biol. 2016; 17:240–56. https://doi.org/10.1038/nrm.2015.16 PMID:26790531

11. Holen HL, Shadidi M, Narvhus K, Kjøsnes O, Tierens A, Aasheim HC. Signaling through ephrin-a ligand leads to activation of Src-family kinases, Akt phosphorylation, and inhibition of antigen receptor-induced apoptosis. J Leukoc Biol. 2008; 84:1183–91. https://doi.org/10.1189/jlb.1207829 PMID:18593733

12. Miao H, Wei BR, Peehl DM, Li Q, Alexandrou T, Schelling JR, Rhim JS, Sedor JR, Burnett E, Wang B. Activation of EphA receptor tyrosine kinase inhibits the Ras/MAPK pathway. Nat Cell Biol. 2001; 3:527–30. https://doi.org/10.1038/35074604 PMID:11331884

13. Davy A, Robbins SM. ephrin-A5 modulates cell adhesion and morphology in an integrin-dependent manner. EMBO J. 2000; 19:5396–405. https://doi.org/10.1093/emboj/19.20.5396 PMID:11032807

14. Wu J, Luo H. Recent advances on T-cell regulation by receptor tyrosine kinases. Curr Opin Hematol. 2005; 12:292–97. https://doi.org/10.1097/01.moh.0000166497.26397.9f PMID:15928486

15. Pfaff D, Fiedler U, Augustin HG. Emerging roles of the Angiopoietin-Tie and the ephrin-Eph systems as regulators of cell trafficking. J Leukoc Biol. 2006; 80:719–26. https://doi.org/10.1189/jlb.1105652 PMID:16864601

16. Campbell TN, Robbins SM. The Eph receptor/ephrin system: an emerging player in the invasion game. Curr Issues Mol Biol. 2008; 10:61–66. PMID:18525107

17. Yang WH, Cha JH, Xia W, Lee HH, Chan LC, Wang YN, Hsu JL, Ren G, Hung MC. Juxtacrine signaling inhibits antitumor immunity by upregulating PD-L1 expression. Cancer Res. 2018; 78:3761–68. https://doi.org/10.1158/0008-5472.CAN-18-0040 PMID:29789418

18. Ayers M, Lunceford J, Nebozhyn M, Murphy E, Loboda A, Kaufman DR, Albright A, Cheng JD, Kang SP, Shankaran V, Piha-Paul SA, Yearley J, Seiwert TY, et al. IFN-γ-related mRNA profile predicts clinical response to PD-1 blockade. J Clin Invest. 2017; 127:2930–40. https://doi.org/10.1172/JCI91190 PMID:28650338

19. Teng MW, Ngiow SF, Ribas A, Smyth MJ. Classifying cancers based on T-cell infiltration and PD-L1. Cancer Res. 2015; 75:2139–45. https://doi.org/10.1158/0008-5472.CAN-15-0255 PMID:25977340

20. Boussiotis VA. Molecular and biochemical aspects of the PD-1 checkpoint pathway. N Engl J Med. 2016; 375:1767–78. https://doi.org/10.1056/NEJMra1514296 PMID:27806234

21. Wang W, Chapman NM, Zhang B, Li M, Fan M, Laribee RN, Zaidi MR, Pfeffer LM, Chi H, Wu ZH. Correction: upregulation of PD-L1 via HMGB1-activated IRF3 and NF-κB contributes to UV radiation-induced immune suppression. Cancer Res. 2019; 79:5682. https://doi.org/10.1158/0008-5472.CAN-19-2862 PMID:31676679

22. Wang X, Li M. Correlate tumor mutation burden with immune signatures in human cancers. BMC Immunol. 2019; 20:4. https://doi.org/10.1186/s12865-018-0285-5 PMID:30634925

23. Lamm N, Maoz K, Bester AC, Im MM, Shewach DS, Karni R, Kerem B. Folate levels modulate oncogene-induced replication stress and tumorigenicity. EMBO Mol Med. 2015; 7:1138–52. https://doi.org/10.15252/emmm.201404824 PMID:26197802

24. Hellmann MD, Nathanson T, Rizvi H, Creelan BC, Sanchez-Vega F, Ahuja A, Ni A, Novik JB, Mangarin LM, Abu-Akeel M, Liu C, Sauter JL, Rekhtman N, et al. Genomic features of response to combination immunotherapy in patients with advanced non-small-cell lung cancer. Cancer Cell. 2018; 33:843–52.e4. https://doi.org/10.1016/j.ccell.2018.03.018 PMID:29657128

25. Huusko P, Ponciano-Jackson D, Wolf M, Kiefer JA, Azorsa DO, Tuzmen S, Weaver D, Robbins C, Moses T, Allinen M, Hautaniemi S, Chen Y, Elkahloun A, et al. Nonsense-mediated decay microarray analysis identifies mutations of EPHB2 in human prostate cancer. Nat Genet. 2004; 36:979–83. https://doi.org/10.1038/ng1408 PMID:15300251

26. Kumar SR, Masood R, Spannuth WA, Singh J, Scehnet J, Kleiber G, Jennings N, Deavers M, Krasnoperov V, Dubeau L, Weaver FA, Sood AK, Gill PS. The receptor tyrosine kinase EphB4 is overexpressed in ovarian cancer, provides survival signals and predicts poor outcome. Br J Cancer. 2007; 96:1083–91. https://doi.org/10.1038/sj.bjc.6603642 PMID:17353927

27. Kang JU, Koo SH, Kwon KC, Park JW, Kim JM. Identification of novel candidate target genes, including EPHB3, MASP1 and SST at 3q26.2-q29 in squamous cell carcinoma of the lung. BMC Cancer. 2009; 9:237. https://doi.org/10.1186/1471-2407-9-237 PMID:19607727

28. Chen DS, Mellman I. Oncology meets immunology: the cancer-immunity cycle. Immunity. 2013; 39:1–10. https://doi.org/10.1016/j.immuni.2013.07.012 PMID:23890059

29. Chiari R, Hames G, Stroobant V, Texier C, Maillère B, Boon T, Coulie PG. Identification of a tumor-specific shared antigen derived from an Eph receptor and presented to CD4 T cells on HLA class II molecules. Cancer Res. 2000; 60:4855–63. PMID:10987298

30. Tatsumi T, Herrem CJ, Olson WC, Finke JH, Bukowski RM, Kinch MS, Ranieri E, Storkus WJ. Disease stage variation in CD4+ and CD8+ T-cell reactivity to the receptor tyrosine kinase EphA2 in patients with renal cell carcinoma. Cancer Res. 2003; 63:4481–89. PMID:12907621

31. Sharfe N, Freywald A, Toro A, Dadi H, Roifman C. Ephrin stimulation modulates T cell chemotaxis. Eur J Immunol. 2002; 32:3745–55.

https://doi.org/10.1002/1521-4141(200212)32:12<3745::AID-IMMU3745>3.0.CO;2-M PMID:12516569

32. Aasheim HC, Delabie J, Finne EF. ephrin-A1 binding to CD4+ T lymphocytes stimulates migration and induces tyrosine phosphorylation of PYK2. Blood. 2005; 105:2869–76. https://doi.org/10.1182/blood-2004-08-2981 PMID:15585656

33. Holen HL, Nustad K, Aasheim HC. Activation of EphA receptors on CD4+CD45RO+ memory cells stimulates migration. J Leukoc Biol. 2010; 87:1059–68. https://doi.org/10.1189/jlb.0709497 PMID:20160140

34. Tokunaga R, Zhang W, Naseem M, Puccini A, Berger MD, Soni S, McSkane M, Baba H, Lenz HJ. CXCL9, CXCL10, CXCL11/CXCR3 axis for immune activation - a target for novel cancer therapy. Cancer Treat Rev. 2018; 63:40–47. https://doi.org/10.1016/j.ctrv.2017.11.007 PMID:29207310

35. Socinski MA, Jotte RM, Cappuzzo F, Orlandi F, Stroyakovskiy D, Nogami N, Rodríguez-Abreu D, Moro-Sibilot D, Thomas CA, Barlesi F, Finley G, Kelsch C, Lee A, et al, and IMpower150 Study Group. Atezolizumab for first-line treatment of metastatic nonsquamous NSCLC. N Engl J Med. 2018; 378:2288–301. https://doi.org/10.1056/NEJMoa1716948 PMID:29863955

36. Herbst RS, Soria JC, Kowanetz M, Fine GD, Hamid O, Gordon MS, Sosman JA, McDermott DF, Powderly JD, Gettinger SN, Kohrt HE, Horn L, Lawrence DP, et al. Predictive correlates of response to the anti-PD-L1 antibody MPDL3280A in cancer patients. Nature. 2014; 515:563–67. https://doi.org/10.1038/nature14011 PMID:25428504

37. Newman AM, Liu CL, Green MR, Gentles AJ, Feng W, Xu Y, Hoang CD, Diehn M, Alizadeh AA. Robust enumeration of cell subsets from tissue expression profiles. Nat Methods. 2015; 12:453–57. https://doi.org/10.1038/nmeth.3337 PMID:25822800

38. Charoentong P, Finotello F, Angelova M, Mayer C, Efremova M, Rieder D, Hackl H, Trajanoski Z. Pan-cancer immunogenomic analyses reveal genotype-immunophenotype relationships and predictors of response to checkpoint blockade. Cell Rep. 2017; 18:248–62. https://doi.org/10.1016/j.celrep.2016.12.019 PMID:28052254

39. Thorsson V, Gibbs DL, Brown SD, Wolf D, Bortone DS, Ou Yang TH, Porta-Pardo E, Gao GF, Plaisier CL, Eddy JA, Ziv E, Culhane AC, Paull EO, et al, and Cancer Genome Atlas Research Network. The immune landscape of cancer. Immunity. 2018; 48:812–30.e14. https://doi.org/10.1016/j.immuni.2018.03.023 PMID:29628290

40. Sanchez-Vega F, Mina M, Armenia J, Chatila WK, Luna A, La KC, Dimitriadoy S, Liu DL, Kantheti HS, Saghafinia S, Chakravarty D, Daian F, Gao Q, et al, and Cancer Genome Atlas Research Network. Oncogenic signaling pathways in the cancer genome atlas. Cell. 2018; 173:321–37.e10. https://doi.org/10.1016/j.cell.2018.03.035 PMID:29625050

41. Jiang T, Li X, Wang J, Su C, Han W, Zhao C, Wu F, Gao G, Li W, Chen X, Li J, Zhou F, Zhao J, et al. Mutational landscape of cfDNA identifies distinct molecular features associated with therapeutic response to first-line platinum-based doublet chemotherapy in patients with advanced NSCLC. Theranostics. 2017; 7:4753–62. https://doi.org/10.7150/thno.21687 PMID:29187901

42. Lai Z, Markovets A, Ahdesmaki M, Chapman B, Hofmann O, McEwen R, Johnson J, Dougherty B, Barrett JC, Dry JR. VarDict: a novel and versatile variant caller for next-generation sequencing in cancer research. Nucleic Acids Res. 2016; 44:e108. https://doi.org/10.1093/nar/gkw227 PMID:27060149

43. Wang K, Li M, Hakonarson H. ANNOVAR: functional annotation of genetic variants from high-throughput sequencing data. Nucleic Acids Res. 2010; 38:e164. https://doi.org/10.1093/nar/gkq603 PMID:20601685

44. Chalmers ZR, Connelly CF, Fabrizio D, Gay L, Ali SM, Ennis R, Schrock A, Campbell B, Shlien A, Chmielecki J, Huang F, He Y, Sun J, et al. Analysis of 100,000 human cancer genomes reveals the landscape of tumor mutational burden. Genome Med. 2017; 9:34. https://doi.org/10.1186/s13073-017-0424-2 PMID:28420421

45. Bolger AM, Lohse M, Usadel B. Trimmomatic: a flexible trimmer for illumina sequence data. Bioinformatics. 2014; 30:2114–20. https://doi.org/10.1093/bioinformatics/btu170 PMID:24695404

46. Li X, Nair A, Wang S, Wang L. Quality control of RNA-seq experiments. Methods Mol Biol. 2015; 1269:137–46. https://doi.org/10.1007/978-1-4939-2291-8_8 PMID:25577376

47. Langmead B, Salzberg SL. Fast gapped-read alignment with bowtie 2. Nat Methods. 2012; 9:357–59. https://doi.org/10.1038/nmeth.1923 PMID:22388286

48. Kim D, Langmead B, Salzberg SL. HISAT: a fast spliced aligner with low memory requirements. Nat Methods. 2015; 12:357–60. https://doi.org/10.1038/nmeth.3317 PMID:25751142

49. Liao Y, Smyth GK, Shi W. featureCounts: an efficient general purpose program for assigning sequence reads to genomic features. Bioinformatics. 2014; 30:923–30. https://doi.org/10.1093/bioinformatics/btt656 PMID:24227677

SUPPLEMENTARY MATERIALS

Supplementary Figure

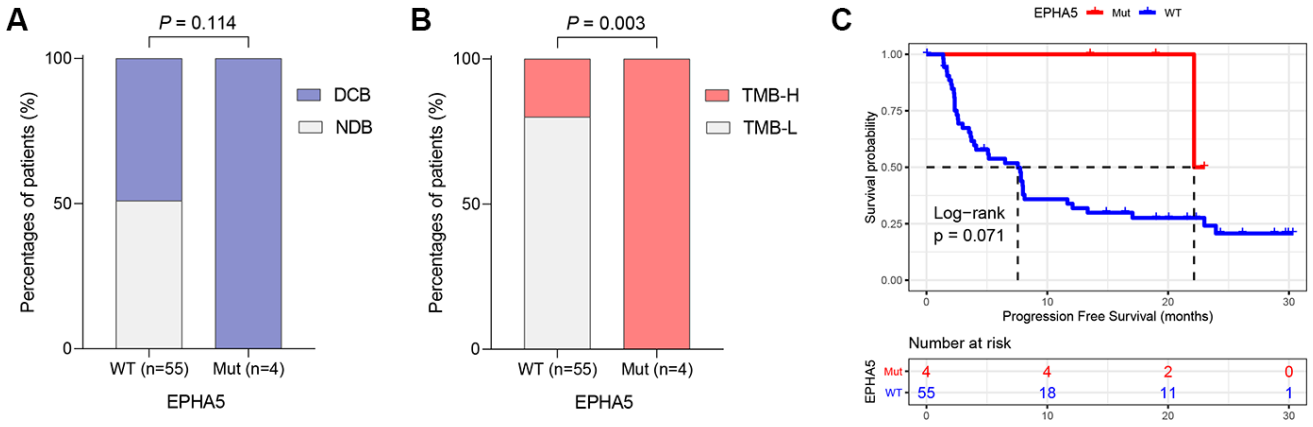

Supplementary Figure 1. Non-squamous NSCLC patients with EPHA5 mutation had better clinical response and outcome after ICI therapy. All patients with EPHA5 mutations (**A**) presented durable clinical benefit to ICIs, and (**B**) had high TMB. (**C**) The EPHA5-Mut group tended to have longer PFS than the EPHA5-WT group.

Supplementary Tables

Supplementary Table 1. Clinical characteristics of the studied LUAD patients from Hellmann cohort.

Characteristics	All patients	EPHA5 Mut	EPHA5 WT	P value
Total (cases)	59	4	55	
Gender [cases (%)]				0.624
Male	22 (37.3)	2 (50.0)	20 (36.4)	
Female	37 (62.7)	2 (50.0)	35 (63.6)	
Age (years)				0.148
Median	63	56.5	66	
IQR	56.00-70.50	52.25-61.25	56.50-71.00	
Smoking status [cases (%)]				0.566
Current/former	46 (78.0)	4 (100.0)	42 (76.4)	
Never	13 (22.0)	0 (0.0)	13 (23.6)	
Performance status [cases (%)]				1
ECOG_0	28 (47.5)	2 (50.0)	26 (47.3)	
ECOG_1	31 (52.5)	2 (50.0)	29 (52.7)	
Clinical benefit [cases (%)]				0.114
DCB	31 (52.5)	4 (100.0)	27 (49.1)	
NDB	28 (47.5)	0 (0.0)	28 (50.9)	

DCB: durable clinical benefit, NDB: no durable benefit;
P value: Wilcoxon test rank sum or Fisher's exact test (two sided) was used for the comparison between the EPHA5 Mut and WT groups.

Supplementary Table 2. DDR core pathway membership.

Base Excision Repair (BER)	Nucleotide Excision Repair (NER, including TC-NER and GC-NER))	Mismatch Repair (MMR)	Fanconi Anemia (FA)	Homologous Recombination (HR)	Non-homologous End Joining (NHEJ)	Direct Repair (DR)	Translesion Synthesis (TLS)	Damage Sensor etc.
PARP1	CUL5	EXO1	FANCA	MRE11A	LIG4	ALKBH2	POLN	ATM
POLB	ERCC1	MLH1	FANCB	NBN	NHEJ1	ALKBH3	POLQ	ATR
APEX1	ERCC2	MLH3	FANCC	RAD50	POLL	MGMT	REV1	ATRIP
APEX2	ERCC4	MSH2	FANCD2	TP53BP1	POLM		REV3L	CHEK1
FEN1	ERCC5	MSH3	FANCI	XRCC2	PRKDC		SHPRH	CHEK2
TDG	ERCC6	MSH6	FANCL	XRCC3	XRCC4			MDC1
TDP1	POLE	PMS1	FANCM	BARD1	XRCC5			RNMT
UNG	POLE3	PMS2	UBE2T	BLM	XRCC6			TOPBP1
	XPA			BRCA1				TREX1
	XPC			BRCA2				
				BRIP1				
				EME1				
				GEN1				
				MUS81				
				PALB2				
				RAD51				
				RAD52				
				RBBP8				
				SHFM1				
				SLX1A				
				TOP3A				

Supplementary Table 3. Clinical characteristics of the studied LUAD patients from MSKCC immunotherapy cohort.

Characteristics	All patients	EPHA5 Mut	EPHA5 WT	P value
Total (cases)	271	23	248	
Gender [cases (%)]				0.827
Male	117 (43.2)	9 (39.1)	108 (43.5)	
Female	154 (56.8)	14 (60.9)	140 (56.5)	
Age Group at Diagnosis in Years [cases (%)]				0.55
31-50	28 (10.3)	2 (8.7)	26 (10.5)	
50-60	61 (22.5)	8 (34.8)	53 (21.4)	
61-70	85 (31.4)	6 (26.1)	79 (31.9)	
>71	97 (35.8)	7 (30.4)	90 (36.3)	
Drug Type [cases (%)]				0.634
PD-1/PDL-1	255 (94.1)	21 (91.3)	234 (94.4)	
Combo	16 (5.9)	2 (8.7)	14 (5.6)	

P value: Fisher's exact test (two sided) was used for the comparison between the EPHA5 Mut and WT groups

Supplementary Table 4. Clinical characteristics of the studied LUAD patients from Chinese cohort.

Characteristics	All patients	EPHA5 Mut	EPHA5 WT	P value
Total (cases)	143	9	134	
Gender [cases (%)]				0.086
Male	86 (60.1)	8 (88.9)	78 (58.2)	
Female	57 (39.9)	1 (11.1)	56 (41.8)	
Age (years)				0.206
Median	62.00	66.00	62.00	
IQR	55.00-68.00	63.00-67.00	54.25-68.00	
Smoking status [cases (%)]				0.140
Current/former	58 (40.6)	6 (66.7)	52 (38.8)	
Never	70 (49.0)	2 (22.2)	68 (50.7)	
NA	15 (10.5)	1 (11.1)	14 (10.4)	
Pathological stage [cases (%)]				0.921
I	16 (11.2)	1 (11.1)	15 (11.2)	
II	27 (18.9)	2 (22.2)	25 (18.7)	
III	59 (41.2)	3 (33.3)	56 (41.8)	
IV	41 (28.7)	3 (33.4)	38 (28.3)	

NA: not available;

P value: Wilcoxon test rank sum or Fisher's exact test (two sided) was used for the comparison between the EPHA5 Mut and WT groups, and NA was not included in the statistical analysis

Supplementary Table 5. Gene list of the designed NGS panel.

Hugo Symbol	Hugo Symbol	Hugo Symbol	Hugo Symbol	Hugo Symbol	Hugo Symbol	Hugo Symbol
AMER1	IPO7	CREBBP	PDCD1LG2	HSPA4	ESR1	DHFR
ASXL1	MED19	CRKL	PDGFRB	CNOT8	ETV6	GSTA1
ATRX	MARK2	CRLF2	PIK3C2G	GABRP	FANCA	SOD2
AURKB	ANO1	CSF1R	PIK3CB	F13A1	FBXW7	SLC22A2
BCOR	KDM5A	CSF3R	PIK3CG	FLOT1	FGF19	SEMA3C
BRD4	ZDHHC17	CXCR4	PIK3R1	HSPA1B	FGF3	ABCB1
CBFB	VSIG10	CYLD	PIK3R2	MAP3K4	FGF4	SLC31A1
CDC73	CTAGE5	DAXX	PLCG2	TRA2A	FGFR1	HSPA5
CDK12	PRPF39	DICER1	PPARG	ABCA13	FGFR2	CYP2C19
CDK8	MAP4K5	DIS3	PPP2R1A	CALD1	FGFR3	CYP2C8
CIC	ARID4A	DOT1L	PRKCI	UBE3C	FH	SLIT1
CTCF	TECPR2	EP300	PTCH1	MMP16	FLT1	ABCC2
FAM46C	APOPT1	EPHA3	PTPN11	RIPK2	HRAS	RRM1
FAT1	HAUS2	EPHA5	RAD51	RAD21	IDH1	GSTP1
FOXL2	ATP9B	EPHA7	RAD51B	IARS	IDH2	SLCO1B3
FUBP1	SPC24	EPHB1	RAD52	MAPKAP1	JAK1	SLCO1B1
GATA1	MYADM	ERBB4	RAD54L	UPF2	JAK2	CYP19A1
GATA2	KIR3DX1	ERG	RAF1	PDE6C	KRAS	CYBA
IKZF1	ZNF805	ETV1	RARA	ADRB1	MAP2K1	TYMS
KDM5C	C20orf96	EZH2	RPTOR	ACADSB	MDM2	CYP2B6
LMO1	NCOA6	FANCC	RUNX1	TPH1	MDM4	XRCC1
MYCL	TMPRSS15	FANCG	SDHA	PTPRJ	MEN1	ERCC2
NKX2-1	DSCAM	FAS	SETD2	FOLH1	MET	ERCC1
PRDM1	RRP1B	FGFR4	SF3B1	ALG9	MLH1	HNF4A
PREX2	C22orf23	FLCN	SMAD2	HYOU1	MRE11A	CBR3
RBM10	MOV10L1	FLT3	SMAD3	MAGOHB	MSH3	CYP2D6
RNF43	WWC3	FLT4	SMARCA4	TXNRD1	MSH6	GSTM1
SPEN	ARHGAP6	FOXP1	SMARCB1	HCAR2	MTOR	EWSR1
TET2	BCYRN1	GATA3	SMO	EXOSC8	MUTYH	FUS
TOP1	ZNF711	GLI1	SOCS1	TNFSF13B	NBN	HEY1
PDPN	TBC1D8B	GNA11	SOX2	SNX6	NF2	NR4A3
GMEB1	DOCK11	GNA13	SOX9	AK7	NOTCH1	PDGFB
MTF1	LONRF3	GNAQ	SPOP	CYFIP1	NRAS	SS18
ZZZ3	KIAA1210	GNAS	SRC	GANC	NT5C2	EML4
RABGAP1L	ARHGAP4	GRIN2A	STAT3	NEO1	NTRK1	CD74
IRF6	BAP1	GSK3B	SUFU	FANCI	NTRK2	SLC34A2
PLEKHH2	DDR2	H3F3A	SYK	ITGAL	NTRK3	KIF5B
PNO1	ERRFI1	HGF	TBX3	ARMC5	PALB2	RIC1
TSN	NPM1	HNF1A	TGFBR2	NUP93	PBRM1	AGPAT9
ARL6IP6	ROS1	ID3	TMPRSS2	IRF8	PDGFRA	CAST
NAB1	NR1I3	IGF1R	TNFAIP3	NF1	PIK3CA	ZMYM4
ALS2CR11	OTOS	IGF2	TNFRSF14	RHOT1	PMS2	SLC30A5
ULK4	C8orf34	IKBKE	TSHR	TAF15	POLD1	CEP120
KPNA4	NAB2	IL7R	U2AF1	KPNB1	POLE	C5orf15
ZBBX	PPHLN1	INHBA	WHSC1	ABCA8	PRKAR1A	SIMC1
LRRC34	ABL1	INPP4B	WHSC1L1	KCNJ2	PTEN	PGBD1
SEL1L3	AKT2	IRF4	XPO1	NUP85	RAC1	HAUS6
NFXL1	AKT3	IRS2	CXCL8	LAMA3	RAD50	ZNF367
SHROOM3	ALOX12B	JAK3	EIF4G3	MALT1	RAD51C	SFXN4
FRAS1	ARID1A	JUN	STMN1	CDC25B	RAD51D	CEP290
CBR4	ARID1B	KDM6A	LEPR	CD40	RB1	STYX
GPM6A	ARID2	KDR	ASH1L	FGF16	RET	MAPKBP1
FAM149A	ATR	KEAP1	FMO1	RPA4	RICTOR	ZNF91
MTRR	AURKA	KMT2A	SIPA1L2	STAG2	SDHB	APOL2

C5orf42	AXIN1	KMT2C	RYR2	BRS3	SDHC	NKAP
ADAMTS6	AXL	KMT2D	ADSS	IRAK1	SDHD	DBT
BTF3	BARD1	LYN	ID2	AKT1	SMAD4	DIAPH1
ANKRA2	BCL2	MAP2K2	CALM2	ALK	STK11	HLA-DRB1
CHD1	BCL2L1	MAP2K4	MSH2	APC	TERT	COL15A1
CDKL3	BTG1	MAP3K1	PAPOLG	AR	TP53	WDR5
PURA	BTK	MCL1	REL	ARAF	TSC1	MMP3
RBM27	CALR	MED12	MEIS1	ATM	TSC2	NLRP7
FAM153B	CARD11	MEF2B	MRPL19	BLM	VEGFA	DEPDC5
HNRNPH1	CASP8	MITF	SUCLG1	BRAF	VHL	DYNC2H1
ACOT13	CBL	MPL	UBE2E3	BRCA1	WT1	STARD4
PAQR8	CCND2	MYC	NDUFS1	BRCA2	PIGF	ZNF2
SASH1	CCND3	MYCN	ARPC2	BRIP1	B2M	TOE1
CNKSR3	CCNE1	MYD88	CUL3	CCND1	MAPK1	EZR
TAGAP	CD274	NFE2L2	CAB39	CDH1	MTHFR	HLA-A
TNRC18	CD79A	NFKBIA	FANCD2	CDK4	CDA	HLA-B
SUGCT	CD79B	NOTCH2	TOP2B	CDKN2A	DPYD	HLA-C
TRIM24	CDK6	NOTCH3	CCR4	CHEK2	MTR	SLC7A8
ERI1	CDKN1A	NSD1	KIT	CTNNB1	GALNT14	RFC1
TNKS	CDKN1B	P2RY8	COX18	DNMT3A	LRP2	STRBP
TMEM67	CDKN2B	PARK2	MYO10	EGFR	ATIC	PLEKHA1
RNF19A	CDKN2C	PARP1	DROSHA	ERBB2	UGT1A1	
ANKRD46	CEBPA	PAX5	CDK7	ERBB3	XPC	
C9orf72	CHEK1	PDCD1	CDO1	ERCC4	UMPS	